J Mater Sci (2007) 42:9316–9323
DOI 10.1007/s10853-007-1909-y

Synthesis and analysis of CuS with different morphologies using cyclic microwave irradiation

Titipun Thongtem · Anukorn Phuruangrat · Somchai Thongtem

Received: 10 March 2007 / Accepted: 31 May 2007 / Published online: 28 July 2007

Abstract Nano- and micro-sized CuS crystals were successfully synthesized from copper and sulfur sources ($CuCl_2 \cdot 2H_2O$, CuBr, $Cu(CH_3COO)_2 \cdot H_2O$, CH_3CSNH_2, $NH_2CSNHNH_2$ and NH_2CSNH_2) in ethylene glycol assisted by the cyclic irradiation of different microwave powers and prolonged times. By using XRD and SAED, CuS (hcp) was detected. The products characterized using SEM and TEM compose of assemblies of nano-flakes, clusters of nano-particles, nano-fibers, nano-rods and sponge-like structures influenced by the synthesized conditions. Their lattice vibrations are in the same Raman wavenumber at 474 cm^{-1}. Among the different products, the emission peaks are over the range 414–435 nm (2.85–2.99 ev). Reaction evidences of the sources were provided using FTIR. Phase and morphology formations are also proposed on according to the analytical results.

Introduction

Copper sulfides are the IB-VIA compounds. They have a wide varieties of compositions, ranging from S-rich (CuS_2) to Cu-rich (Cu_2S). CuS is an intermediate compound. It is very interesting due to its wide range of applications in optical and electrical devices, such as catalysts, solar cells and cathode materials in lithium rechargeable batteries [1]. It has metallic conduction property, and transforms into a superconductor below the 1.6 K [2]. Recently, copper sulfides with different morphologies have been synthesized. Among them are hollow spheres [1, 3], nanoparticles [4, 5], nanorods [6–8], nanoflakes [9], nanoplates [10], and nanocones and nanobelts [11]. There are different methods used for the synthesis, such as solid-state reaction [7], hydrothermal fabrication [2, 11], sonochemical synthesis [12], photochemical deposition [13] and microwave irradiation [4]. For the present research, nano- and micro-sized CuS crystals with different morphologies such as assemblies of nano-flakes, clusters of nano-sized particles, nano-fibers, nano-rods and sponge-like structures were successfully synthesized from different copper and sulfur sources in ethylene glycol by the cyclic exposure to microwave irradiation. No surfactants were used in the process, which is very simple and novelty.

Experiment

Each of 0.005 mole copper and sulfur sources was dissolved in 30 mL ethylene glycol and stirred for 30 min. The reactions cyclically proceeded using different microwave powers and prolonged times to produce products with different morphologies (Table 1). One cycle of 2 min prolonged time composes of irradiation and non-irradiation for 1 min each. Current temperatures at different microwave powers and prolonged times are shown in Fig. 1. At constant microwave power, the temperatures were increased with the increasing of the prolonged times within about the first 10 min. They tend to be constant afterwards. At the conclusion of the process, the final products were

T. Thongtem (✉)
Department of Chemistry, Faculty of Science, Chiang Mai University, Chiang Mai 50200, Thailand
e-mail: ttpthongtem@yahoo.com; ttpthongtem@hotmail.com

A. Phuruangrat · S. Thongtem
Department of Physics, Faculty of Science, Chiang Mai University, Chiang Mai 50200, Thailand

Table 1 Copper and sulfur sources, product codes and morphologies at different conditions

Copper and sulfur sources	Power (W)	Prolonged time (min)	Product codes	Morphologies
$CuCl_2 \cdot 2H_2O + CH_3CSNH_2$	180	10	CA1	Assemblies of nano-flakes (Micro-sized flowers)
	180	20	CA2	
	180	30	CA3	
	180	40	CA4	
	300	10	CA5	
	450	10	CA6	
	600	10	CA7	
$CuCl_2 \cdot 2H_2O + CH_3CSNH_2$	600	20	CA	Assemblies of nano-flakes (Micro-sized flowers)
$CuCl_2 \cdot 2H_2O + NH_2CSNHNH_2$	600	20	CC	
$CuCl_2 \cdot 2H_2O + NH_2CSNH_2$	600	20	CU	
$CuBr + CH_3CSNH_2$	600	20	BA	Clusters of nano-sized particles
$CuBr + NH_2CSNHNH_2$	600	20	BC	Nano-rods
$CuBr + NH_2CSNH_2$	600	20	BU	Sponge-like structures
$Cu(CH_3COO)_2 \cdot H_2O + CH_3CSNH_2$	600	20	AA	Assemblies of nano-flakes
$Cu(CH_3COO)_2 \cdot H_2O + NH_2CSNHNH_2$	600	20	AC	Nano-fibers
$Cu(CH_3COO)_2 \cdot H_2O + NH_2CSNH_2$	600	20	AU	Clusters of nano-sized particles

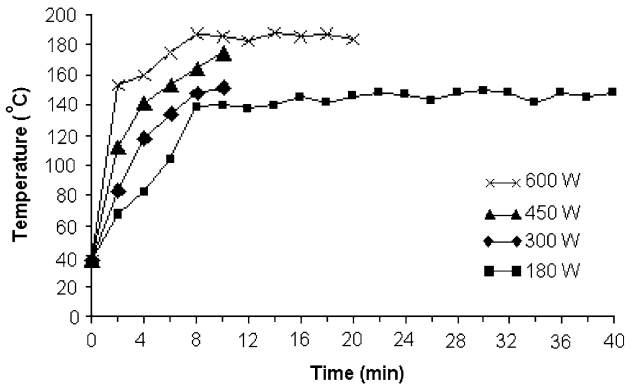

Fig. 1 Current temperatures at different microwave powers and prolonged times used for the present process

washed with water and ethanol, and dried at 80 °C for 12 h. Then, they were characterized using XRD operated at 20 kV, 15 mA and using the Kα line from a Cu target, SEM operated at 15 kV, TEM as well as the use of selected area electron diffraction (SAED) operated at 200 kV, FTIR with KBr as a diluting agent and operated in the range 400–4,000 cm^{-1}, Raman spectrometry using 50 mW Ar Laser with $\lambda = 514.5$ nm, and photoluminescence (PL) spectrometry using a 202 nm exciting wavelength.

Results and discussion

XRD

XRD spectra of the products (Fig. 2) synthesized using different conditions were analyzed and compared with that of the JCPDS software (reference code: 78–0876) [14]. When $CuCl_2 \cdot 2H_2O$ and CH_3CSNH_2 were used as the starting agents, XRD spectra of the products synthesized at different prolonged times and microwave powers revealed the presence of pure CuS (hexagonal) with P63/mmc space group. No characteristic peaks arising from impurities such as CuO and Cu_2S were detected. The XRD peaks became higher and narrower with the increase in the prolonged times and microwave powers. These show that the crystalline products were improved. The prolonged times and microwave powers have the influence on the phase formation by assisting Cu and S atoms in violent vibrating and diffusing (higher amplitude) at longer time. The atoms have the better chance to reside in their normal lattices or in the periodic array. These lead to the increase in the degree or extent of the product crystalline. When one of the copper and sulfur sources were used at constant 20 min prolonged time and 600 W microwave power, pure CuS can be synthesized as well.

Phase formation

During the synthesis, $CuCl_2 \cdot 2H_2O$ reacted with CH_3CSNH_2 in ethylene glycol for several steps and copper complex ($[Cu(CH_3CSNH_2)_2]^{2+}$) formed. Then, the complex was decomposed by microwave irradiation to produce CuS [4]. Due to the existence of crystal water in $CuCl_2 \cdot 2H_2O$ and trace water in ethylene glycol, CH_3CSNH_2 reacted with H_2O to form H_2S. Subsequently, H_2S was decomposed by the microwave irradiation [15, 16]. S^{2-} generated and further reacted with Cu^{2+} to produce CuS.

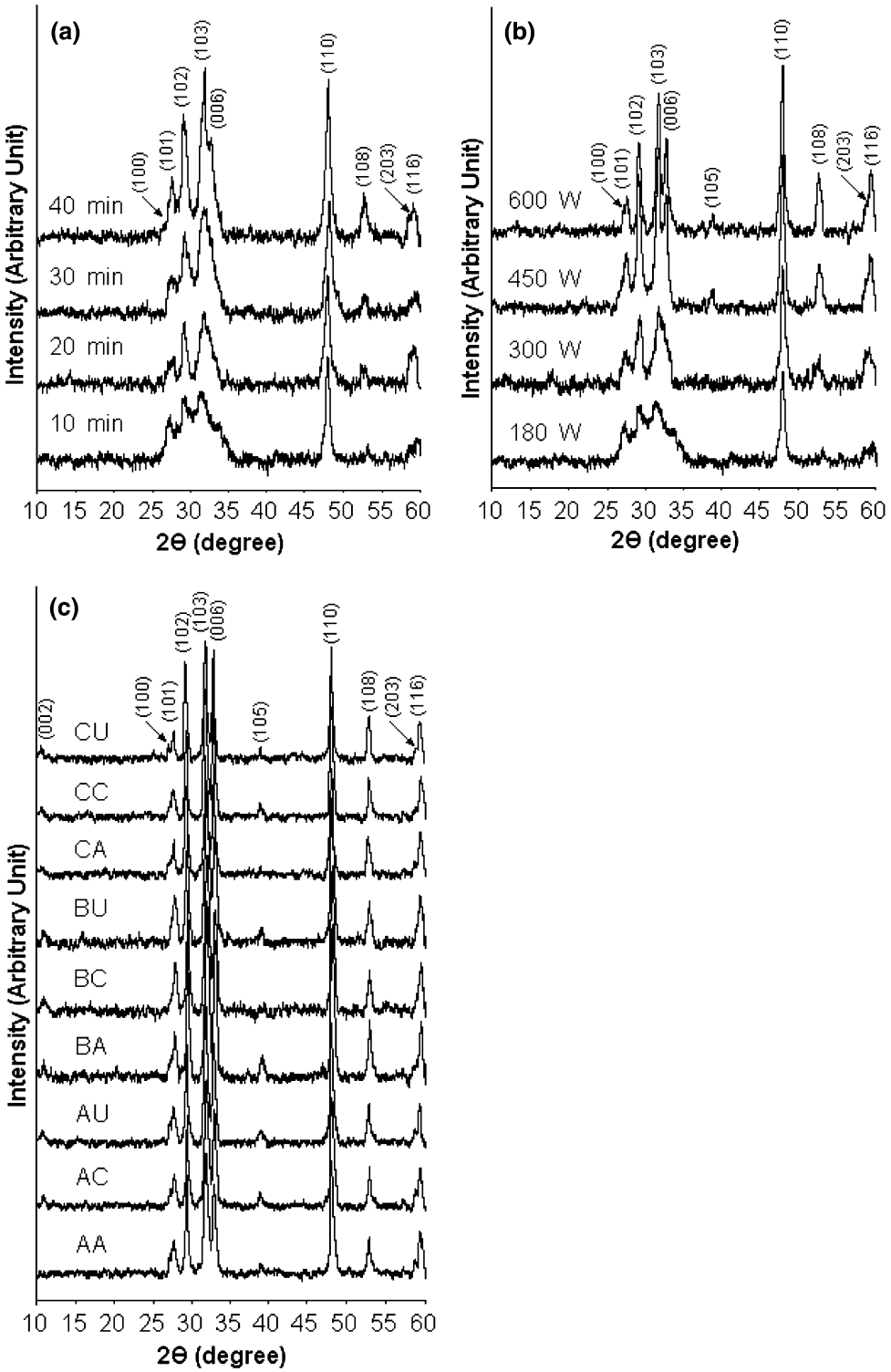

Fig. 2 XRD spectra of the products synthesized using different conditions (starting agents/microwave powers/prolonged times). (**a**) $CuCl_2{\cdot}2H_2O$ and CH_3CSNH_2/180 W/10–40 min, (**b**) $CuCl_2{\cdot}2H_2O$ and CH_3CSNH_2/180-600 W/10 min, and (**c**) different starting agents/600 W/20 min

The reactions were similar to the above when $CuCl_2 \cdot 2H_2O$ was replaced by $Cu(CH_3COO)_2 \cdot H_2O$, and CH_3CSNH_2 by $NH_2CSNHNH_2$ or NH_2CSNH_2. In case of using CuBr as a copper source, Cu^{1+} is not stable in the solution. It can undergo disproportionation in which the oxidation state of Cu^{1+} is simultaneously raised and lowered [17].

$$2Cu^{1+} \longrightarrow Cu^{2+} + Cu^{0}$$

With the assistance of microwave irradiation, Cu^0 was further oxidized to Cu^{2+} by H_2S.

$$Cu^{0} \xrightarrow{\text{Microwave irradiation}} Cu^{2+} + 2e^{-}$$

Cu^{2+} combined with S^{2-} to produce CuS.

$$Cu^{2+} + S^{2-} \xrightarrow{\text{Microwave irradiation}} CuS$$

Reaction evidences between copper and sulfur sources were provided on according to the following. During the synthesizing process, copper and sulfur salts were separately dissolved in ethylene glycol and mixed. The precipitates (copper complexes) formed. Subsequently, they turned into black (CuS) in a microwave oven. In addition, pure thiourea (NH_2CSNH_2) and copper-thiourea complex were characterized using FTIR. Their spectra are shown in Fig. 3. For thiourea spectrum, bands of C = S and C–N stretching vibrations [18, 19], were detected at 735 and 1464 cm^{-1}, respectively. Corresponding bands of the complex were at 697 and 1494 cm^{-1}, respectively. Comparing to thiourea, the first vibration shows red-shift, which was caused by lowering in the wavenumber. It was characterized as the reduced double bond character of carbon and sulfur in the complex. The second is blue-shift due to the greater double bond character of carbon and nitrogen in the complex. It shows the presence of sulfur-copper coordination [19]. Three bands of NH_2 stretching vibrations of thiourea and the complex [19] were the same wavenumber at 3171, 3269 and 3373 cm^{-1}. Their NH_2 bending [18] is also the same wavenumber at 1600 cm^{-1}. The NH_2 stretching and bending vibrations are stationary. In the present case, no bonding between nitrogen and copper is present [18, 19]. Some difference in the intensity peak at 1104 cm^{-1} of thiourea and the complex was detected. When copper-thiourea complex was produced, the intensity peak in thiourea was diminished in the complex. It was influenced by a change in the nature of C = S and C–N bonds due to the complex formation [18].

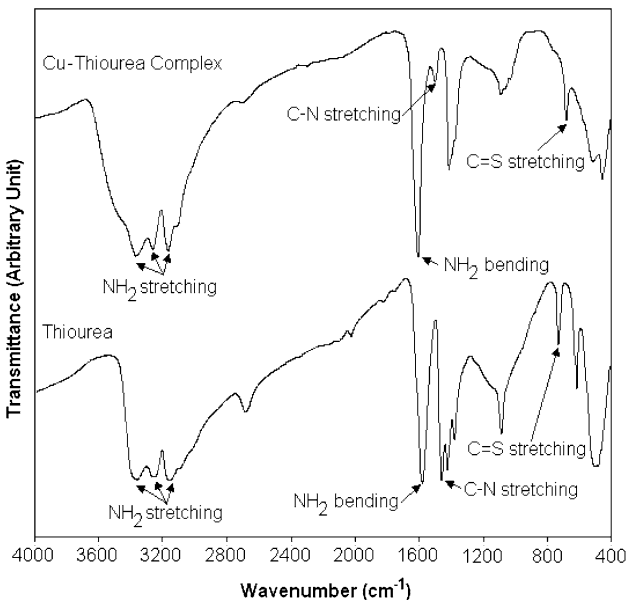

Fig. 3 FTIR spectra of thiourea and copper-thiourea complex

Microwave irradiation is at an advantage over other processes by solving the problems of concentration and temperature gradients in the solution. Its vibration frequency provides uniform condition for the nucleation and growth due to the rapid, uniform and effective heating process. It accelerates the reactions by assisting the decomposition of copper complexes and H_2S, the oxidation and reduction processes, and the formation of CuS.

SEM

Morphologies of the products synthesized using different prolonged times, microwave powers, and starting agents are summarized in Table 1, and SEM images of the selected products are shown in Fig. 4. For the synthesis process using $CuCl_2{\cdot}2H_2O$ and CH_3CSNH_2 as the starting agents at 180 W microwave powers for 10, 20, 30 and 40 min prolonged times, at 300, 450 and 600 W for 10 min, and at 600 W for 20 min, the products (CA1, CA2, CA3, CA4, CA5, CA6, CA7 and CA) are the assemblies of nano-flakes (micro-sized flowers). Both the flowers and flakes became larger at higher power and longer time. The flowers are 4.5 μm in diameters at 600 W and 20 min. A microwave oven supplies energy to the system, which was used to decompose the complexes and accelerate copper sulfide formation. Microwave powers and prolonged times did not have so strong influence on the product shapes as on the sizes.

At constant 600 W for 20 min with the same copper source ($CuCl_2 \cdot 2H_2O$) but different sulfur sources (CH_3CSNH_2, $NH_2CSNHNH_2$ and NH_2CSNH_2), the products (CA, CC and CU) are the assemblies of nano-flakes (micro-sized flowers) although the three sulfur sources are different. They compose of nano-flakes as the fundamental particles. It shows that $CuCl_2 \cdot 2H_2O$ dominated the sulfur sources. Product morphology was influenced by chloride ions in the system. Anions of the copper sources have the influence on growth of the particles. But for those synthesized using CuBr or $Cu(CH_3COO)_2 \cdot H_2O$ as copper sources with different sulfur sources, the products have a variety of morphologies. They are clusters of nano-sized particles, nanorods, sponge-like structures, assemblies of nano-flakes and

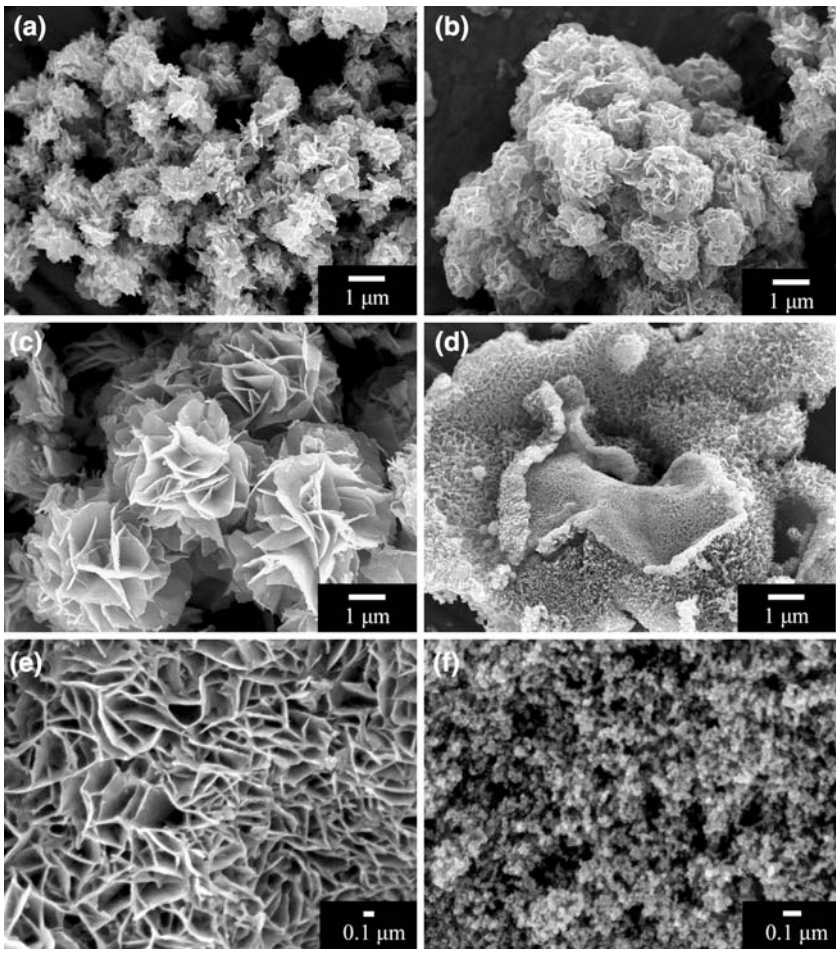

Fig. 4 SEM images of the products. (**a**–**f**) are CA1, CA7, CA, BU, AA and AU, respectively

nano-fibers for BA and AU, BC, BU, AA and AC, respectively. Different product morphologies were influenced by sulfur sources, which have different structure formulas. Nucleation and growth of the particles can play roles in the morphology. The crystal growth of some preferred structure or planes relates to the surface energy of the planes in the specified condition. It is described as the shape selective surface absorption process [20]. The amount of starting agents in the solution also has the influence on different orientation of the particles, which reflects nucleation and growth of the crystals. The orientation was increased with the increasing in the amount of starting agents [21]. Phase with the lowest free energy is thermodynamically stable, and has more chance to exist in the process [22]. This can reflect the product morphologies. Apart from the above, crystal growth is influenced by the solubility of the precursors in the particular solvent and synthesized temperature, which reflects the morphologies [20]. Polarities and boiling points of solvents [23], pH values of the solutions and others can play a role in the shapes and sizes due to the different rates of nucleation and growth.

Different starting agents play a significant role to produce the products with different shapes and sizes, which was influenced by nucleation and growth. They had more role than the microwave irradiation did.

During the formation of CuS, round particles were formed by the assemblage of hcp unit cells. Growths in the x-, y- and z- directions are almost at the same rates. Rod-shaped particles and fibers were formed by stacking up hcp unit cells. There were some unit cells stacked aside as well. To form rods and fibers, growth rate in the z-direction is the fastest. Flake-like particles were formed by the similar process as the rod/fiber formation but growth in the z-direction is the slowest.

The products may contain some imperfect round particles, curved rods/fibers and wavy flakes, due to the microwave vibration frequency, internal stress and others. Different morphologies have the influence on the luminescent property as well.

TEM and SAED

To show more details, the synthesized products were put into a beaker containing ethanol. After ultrasonic vibration,

the liquid was dropped on a copper grid and dried in ambient atmosphere. TEM images and SAED patterns (Fig. 5) of the selected products were characterized and analyzed. They compose of round nano-particles with <20 nm in diameter for BA and AU, nano-rods with <20 nm in diameter for BC, and nano-fibers with as long as 105 nm for AC.

SAED patterns show eight concentric rings corresponding to diffraction planes of the crystalline products. Diameters of the rings were measured from the diffraction patterns on the films. The values of d-spacing of the diffraction planes were calculated [24, 25] and compared with those of the JCPDS software [14]. The diffraction patterns show that the products compose of CuS with hexagonal structure. The analyses interpreted from SAED and XRD patterns are in good accord. The diffraction planes of the products are (100), (103), (006), (105), (110), (108), (203) and (116). The rings are diffuse and hollow showing that the products composed of very fine particles.

Raman analysis

Raman spectra of different products (Fig. 6) are very sharp showing that lattice atoms are arranged in the periodic array. Vibration modes of the crystalline products synthesized from different starting agents are in the same wavenumber at 474 cm^{-1} corresponding to the lattice vibrations. The present results are in accord with those of CuS thin films [26, 27]. Generally, vibration frequency is a parameter controlled by atomic masses, force constant of lattice atoms, atomic bonding and others.

PL spectra

PL emission of CuS dispersed in absolute ethanol (Fig. 7) was determined using a 202 nm (6.14 ev) exciting wavelength. PL spectra of all the products show the broad emission peaks in the range 414–435 nm (2.85–2.99 ev). For each of the copper sources, the spectra show the

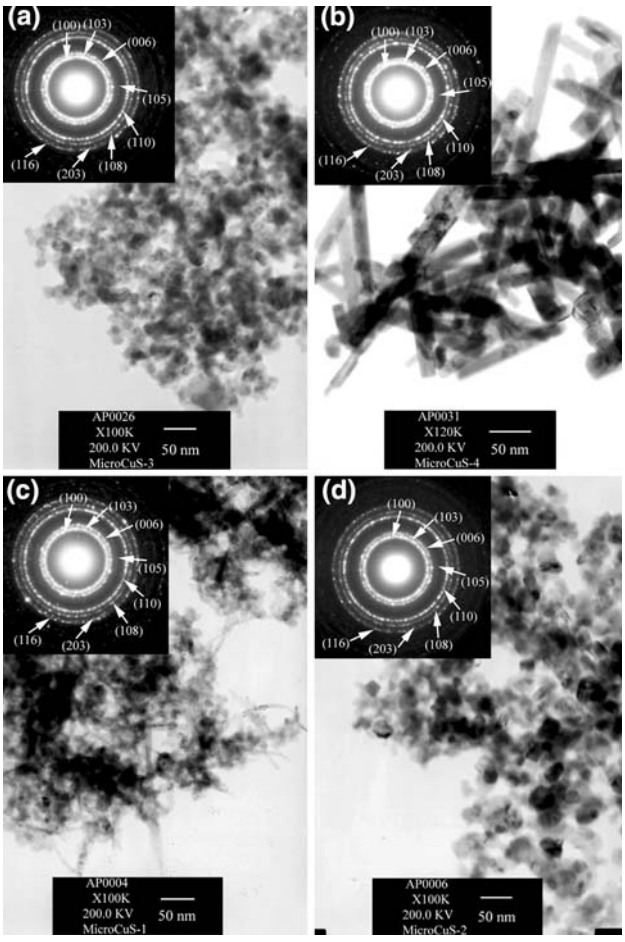

Fig. 5 TEM images and SAED patterns of the products synthesized at 600 W microwave power for 20 min prolonged time. (**a–d**) are BA, BC, AC and AU, respectively

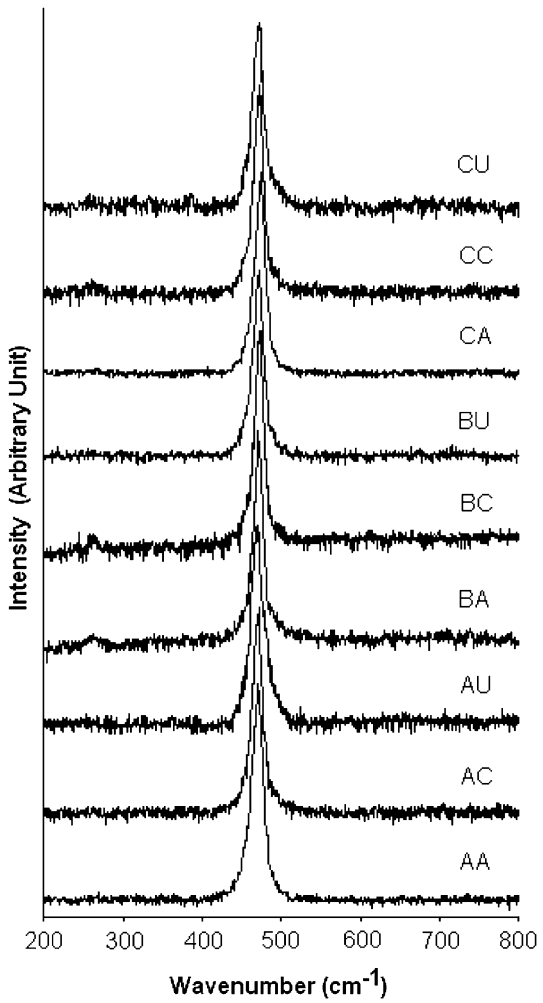

Fig. 6 Raman spectra of the products synthesized using different starting agents at 600 W microwave power for 20 min prolonged time

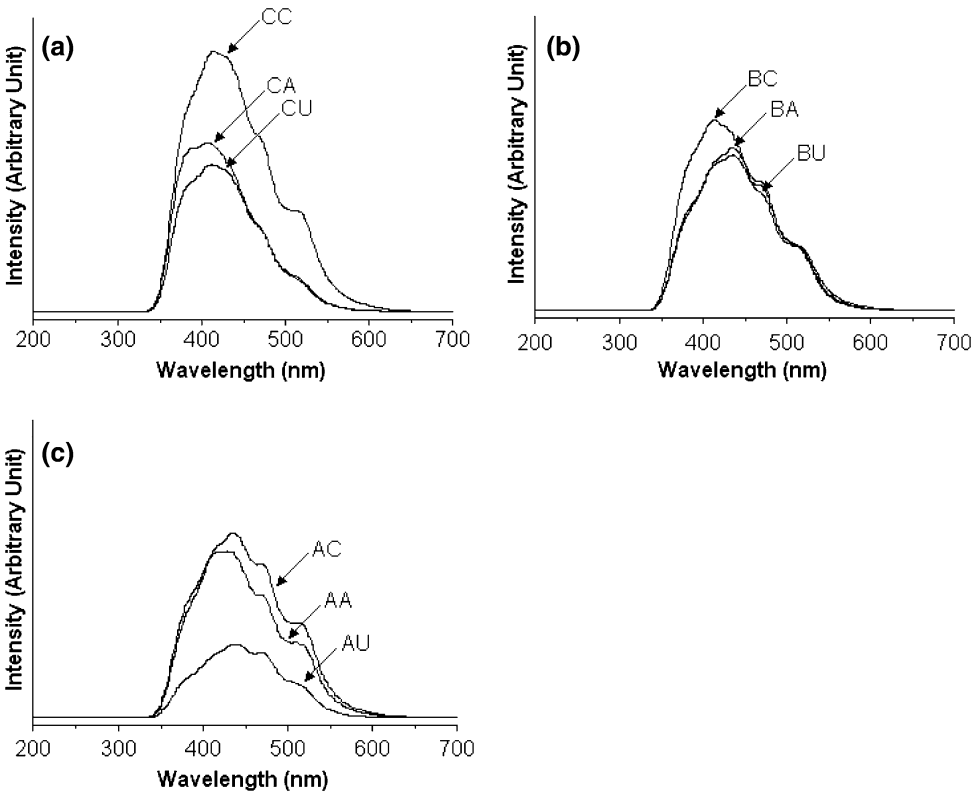

Fig. 7 PL spectra of different products synthesized at 600 W microwave power for 20 min prolonged time. (**a**) CA, CC and CU, (**b**) BA, BC and BU and (**c**) AA, AC and AU

highest intensities at 414 nm (2.99 ev), 414 nm (2.99 ev) and 434 nm (2.86 ev) for the CC, BC and AC products, respectively. The results are in accord with the emission peaks of CuS at 414 nm (2.995 ev) and 437.5 nm (2.834 ev) [28].

Conclusions

Nano- and micro-sized CuS crystals with different morphologies were successfully synthesized by the reactions of different copper and sulfur sources assisted by the cyclic microwave irradiation. The detections of CuS (hcp) phase using XRD and SAED, and of 474 cm^{-1} vibration wavenumber using the Raman spectrometer are in good accord. PL emission peaks of the products are at 414–435 nm (2.85–2.99 ev). Phase and morphology formations are proposed on according to the results characterized using XRD, FTIR, SAED, SEM and TEM.

Acknowledgement We would like to give thank to the Thailand Research Fund, Bangkok Thailand, for funding the research.

References

1. He Y, Yu X, Zhao X (2007) Mater Lett 61:3014
2. Tezuka K, Sheets WC, Kurihara R, Shan YJ, Imoto H, Marks TJ, Poeppelmeier KR (2007) Solid State Sci 9:95
3. Chen X, Wang Z, Wang X, Zhang R, Liu X, Lin W, Qian Y (2004) J Cryst Growth 263:570
4. Chen D, Tang K, Shen G, Sheng J, Fang Z, Liu X, Zheng H, Qian Y (2003) Mater Chem Phys 82:206
5. Ni Y, Liu H, Wang F, Yin G, Hong J, Ma X, Xu Z (2004) Appl Phys A 79:2007
6. Liao XH, Chen NY, Xu S, Yang SB, Zhu JJ (2003) J Cryst Growth 252:593
7. Wang X, Xu C, Zhang Z (2006) Mater Lett 60:345
8. Yang YJ, Xiang JW (2005) Appl Phys A 81:1351
9. Zhang HT, Wu G, Chen XH (2006) Mater Chem Phys 98:298
10. Xu H, Wang W, Zhu W (2006) Mater Lett 60:2203
11. Jiang C, Zhang W, Zou G, Xu L, Yu W, Qian Y (2005) Mater Lett 59:1008
12. Xu JZ, Xu S, Geng J, Li GX, Zhu JJ (2006) Ultrason Sonochem 13:451
13. Podder J, Kobayashi R, Ichimura M (2005) Thin Solid Films 472:71
14. Powder Diffract. File, JCPDS Internat. Centre Diffract. Data, PA 19073–3273, USA, (2001)
15. Huang NM, Kan CS, Khiew PS, Radiman S (2004) J Mater Sci 39:2411. DOI: 10.1023/B: JMSC.0000020003.51378.55
16. Li Y, Huang F, Zhang Q, Gu Z (2000) J Mater Sci 35:5933 DOI: 10.1023/A: 1026714004563
17. Shriver DF, Atkins PW, Overton TL, Rourke JP, Weller MT Armstrong FA (2006) Inorg. Chem, 4th ed., Oxford Univ. Press, p 151
18. Swaminathan K, Irving HMNH (1964) J Inorg Nucl Chem 26:1291
19. Yang J, Zeng JH, Yu SH, Yang L, Zhang YH, Qian YT (2000) Chem Mater 12:2924
20. Biswas S, Kar S, Chaudhuri S (2007) J Cryst Growth 299:94
21. Zhang YC, Hu XY, Qiao T (2004) Solid State Comm 132:779
22. Sopunna K, Thongtem T, McNallan M, Thongtem S (2006) J Mater Sci 41:4654. DOI: 10.1007/s 10853-006-0030-y

23. Lu J, Han Q, Yang X, Lu L, Wang X (2007) Mater Lett 61:2883
24. Thongtem T, Kaowphong S, Thongtem S (2007) J Mater Sci 42:3923
25. Phuruangrat A, Thongtem T, Thongtem S (2007) Mater Lett 61:3805
26. Wang SY, Wang W, Lu ZH (2003) Mater Sci Engin B 103:184
27. Minceva-Sukarova B, Najdoski M, Grozdanov I, Chunnilall CJ (1997) J Molec Struct 410–411:267
28. Ou S, Xie Q, Ma D, Liang J, Hu X, Yu W, Qian Y (2005) Mater Chem Phys 94:460